

SANDIA REPORT

SAND96-8443 • UC-401
Unlimited Release
Printed December 1995

RECEIVED

FEB 29 1996

OSTI

A Reaction Mechanism for Titanium Nitride CVD from $TiCl_4$ and NH_3

(To appear in the proceedings of the Thirteenth International Conference on Chemical Vapor Deposition held May 5-10, 1996 in Los Angeles, CA)

Richard S. Larson and Mark D. Allendorf

Prepared by
Sandia National Laboratories
Albuquerque, New Mexico 87185 and Livermore, California 94551
for the United States Department of Energy
under Contract DE-AC04-94AL85000

Approved for public release; distribution is unlimited.



MASTER

Issued by Sandia National Laboratories, operated for the United States Department of Energy by Sandia Corporation.

NOTICE: This report was prepared as an account of work sponsored by an agency of the United States Government. Neither the United States Government nor any agency thereof, nor any of their employees, nor any of the contractors, subcontractors, or their employees, makes any warranty, express or implied, or assumes any legal liability or responsibility for the accuracy, completeness, or usefulness of any information, apparatus, product, or process disclosed, or represents that its use would not infringe privately owned rights. Reference herein to any specific commercial product, process, or service by trade name, trademark, manufacturer, or otherwise, does not necessarily constitute or imply its endorsement, recommendation, or favoring by the United States Government, any agency thereof or any of their contractors or subcontractors. The views and opinions expressed herein do not necessarily state or reflect those of the United States Government, any agency thereof or any of their contractors or subcontractors.

This report has been reproduced from the best available copy.

Available to DOE and DOE contractors from:

Office of Scientific and Technical Information
P. O. Box 62
Oak Ridge, TN 37831

Prices available from (615) 576-8401, FTS 626-8401

Available to the public from:

National Technical Information Service
U.S. Department of Commerce
5285 Port Royal Rd.
Springfield, VA 22161

DISCLAIMER

**Portions of this document may be illegible
in electronic image products. Images are
produced from the best available original
document.**

SAND96-8443
Unlimited Release
Printed December 1995

**A REACTION MECHANISM FOR TITANIUM NITRIDE CVD
FROM TiCl_4 AND NH_3**

Richard S. Larson and Mark D. Allendorf
Sandia National Laboratories
Livermore, CA 94551-0969

ABSTRACT

A gas-phase and surface reaction mechanism for the CVD of TiN from TiCl_4 and NH_3 is proposed. The only gas-phase process is complex formation, which can compete with deposition. The surface mechanism postulates the stepwise elimination of Cl and H atoms from TiCl_4 and NH_3 , respectively, to form solid TiN and gaseous HCl. The mechanism also accounts for the change in oxidation state of Ti by allowing for liberation of N_2 . Provided that the surface composition is at steady state, the stoichiometry of the overall reaction is reproduced exactly. In addition, the global kinetic law predicted by the mechanism is successfully fit to new deposition data from a rotating disk reactor and is shown to be consistent with literature results.

INTRODUCTION

Thin films of titanium nitride (TiN) have several actual and potential applications in microelectronics, in particular as diffusion barriers between silicon and aluminum layers. While TiN has traditionally been deposited via physical processes such as reactive sputtering, the need for improved step coverage in structures of high aspect ratio has led to the investigation of chemical vapor deposition (CVD) as an alternative. TiN can be deposited from a number of chemical precursor systems, but each has particular disadvantages with regard to integrated circuits. For example, deposition from $\text{TiCl}_4 + \text{N}_2 + \text{H}_2$ requires temperatures that are much too high, while the use of metalorganic compounds such as tetrakis(dimethylamido)titanium (generally in conjunction with NH_3) leads to films that can have significant carbon, oxygen, and hydrogen contamination (1). A compromise of sorts is provided by the $\text{TiCl}_4 + \text{NH}_3$ process, which is feasible at moderate temperatures ($> 750 \text{ K}$) and yields films whose main drawback is chlorine contamination (2). Experimental efforts to improve this process are underway, and the present paper is an attempt to develop a more detailed understanding.

Several quantitative studies of the deposition rate of TiN from TiCl_4 and NH_3 have been reported (3–8), and in two of these (3,4) a global rate law is inferred from the data. In addition, at least one theoretical description of some of the elementary surface processes has appeared (9). To date, however, no attempt has been made to derive an overall rate law from a complete reaction mechanism. In this paper a schematic but self-consistent mechanism is proposed, and an expression for the deposition rate is obtained in terms of the (unknown) individual rate constants. The latter are then evaluated by fitting the predictions of the model to some new experimental data. Finally, the results of this analysis are shown to be generally consistent with the observations of previous investigators.

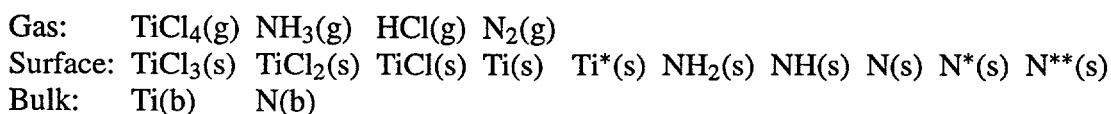
REACTION MODEL

In constructing a mechanism for the TiN CVD process, a few general observations must be taken into account. First, the overall reaction is essentially irreversible at the temperatures normally used, since ΔG is strongly negative for $T > 600 \text{ K}$. Second, there is preliminary evidence (10) that gas-phase reactions are of minor importance in this system, i.e., the process appears to be dominated by surface reactions. A complicating factor is that the titanium atoms undergo a change in oxidation state from +4 to +3. As a consequence, the products of the reaction include (presumably) gas-phase N_2 as well as HCl , and the overall stoichiometry is



The notation (b) is used here to indicate a bulk (solid) species, as distinguished from surface species that function only as reaction intermediates.

A surface mechanism that is consistent with the above observations can now be written in terms of the following species:



The notation for the surface and bulk species requires some elaboration. First of all, a surface species is defined to be one that resides in the topmost layer of the solid, while a bulk species resides in

any layer below this. Furthermore, Ti–N bonds are not explicitly noted here. Thus, for example, $\text{TiCl}_3(\text{s})$ is a surface species in which one of the original Ti–Cl bonds has been replaced by a Ti–N bond. Similarly, in $\text{Ti}(\text{s})$ all four of the Ti–Cl bonds have been replaced. In $\text{Ti}^*(\text{s})$, however, one of the new Ti–N bonds has been severed. The nitrogen-containing species are named analogously, so that in $\text{N}^{**}(\text{s})$ two of the N–Ti bonds have been broken. Keeping in mind the oxidation states in TiN, it is clear that $\text{Ti}^*(\text{s})$ is the immediate precursor to a bulk titanium, $\text{Ti}(\text{b})$, while $\text{N}(\text{s})$ is the species that becomes $\text{N}(\text{b})$. Furthermore, an N_2 molecule is formed from two $\text{N}^{**}(\text{s})$ species by breaking the last N–Ti bond to each. Needless to say, whenever a nitrogen surface species loses a bond, a titanium species must do the same.

In proposing a surface reaction mechanism, we note that the likely interactions among the species defined above fall naturally into five groups:

Titanium deposition:

1. $\text{TiCl}_4(\text{g}) + \text{NH}_2(\text{s}) + \text{Ti}^*(\text{s}) \rightarrow \text{TiCl}_3(\text{s}) + \text{NH}(\text{s}) + \text{HCl}(\text{g}) + \text{Ti}(\text{b})$
2. $\text{TiCl}_4(\text{g}) + \text{NH}(\text{s}) + \text{Ti}^*(\text{s}) \rightarrow \text{TiCl}_3(\text{s}) + \text{N}(\text{s}) + \text{HCl}(\text{g}) + \text{Ti}(\text{b})$

Nitrogen deposition:

3. $\text{TiCl}_3(\text{s}) + \text{NH}_3(\text{g}) + \text{N}(\text{s}) \rightarrow \text{TiCl}_2(\text{s}) + \text{NH}_2(\text{s}) + \text{HCl}(\text{g}) + \text{N}(\text{b})$
4. $\text{TiCl}_2(\text{s}) + \text{NH}_3(\text{g}) + \text{N}(\text{s}) \rightarrow \text{TiCl}(\text{s}) + \text{NH}_2(\text{s}) + \text{HCl}(\text{g}) + \text{N}(\text{b})$
5. $\text{TiCl}(\text{s}) + \text{NH}_3(\text{g}) + \text{N}(\text{s}) \rightarrow \text{Ti}(\text{s}) + \text{NH}_2(\text{s}) + \text{HCl}(\text{g}) + \text{N}(\text{b})$

Surface condensation:

6. $\text{TiCl}_3(\text{s}) + \text{NH}_2(\text{s}) \rightarrow \text{TiCl}_2(\text{s}) + \text{NH}(\text{s}) + \text{HCl}(\text{g})$
7. $\text{TiCl}_3(\text{s}) + \text{NH}(\text{s}) \rightarrow \text{TiCl}_2(\text{s}) + \text{N}(\text{s}) + \text{HCl}(\text{g})$
8. $\text{TiCl}_2(\text{s}) + \text{NH}_2(\text{s}) \rightarrow \text{TiCl}(\text{s}) + \text{NH}(\text{s}) + \text{HCl}(\text{g})$
9. $\text{TiCl}_2(\text{s}) + \text{NH}(\text{s}) \rightarrow \text{TiCl}(\text{s}) + \text{N}(\text{s}) + \text{HCl}(\text{g})$
10. $\text{TiCl}(\text{s}) + \text{NH}_2(\text{s}) \rightarrow \text{Ti}(\text{s}) + \text{NH}(\text{s}) + \text{HCl}(\text{g})$
11. $\text{TiCl}(\text{s}) + \text{NH}(\text{s}) \rightarrow \text{Ti}(\text{s}) + \text{N}(\text{s}) + \text{HCl}(\text{g})$

Bond breaking:

12. $\text{Ti}(\text{s}) + \text{N}(\text{s}) \rightarrow \text{Ti}^*(\text{s}) + \text{N}^*(\text{s})$
13. $\text{Ti}(\text{s}) + \text{N}^*(\text{s}) \rightarrow \text{Ti}^*(\text{s}) + \text{N}^{**}(\text{s})$

N_2 liberation:

14. $2 \text{Ti}(\text{s}) + 2 \text{N}^{**}(\text{s}) + 2 \text{N}(\text{b}) \rightarrow 2 \text{Ti}^*(\text{s}) + \text{N}_2(\text{g}) + 2 \text{N}(\text{s})$

It should be noted that this mechanism (and each step individually) automatically conserves the total number of surface species, or sites. In reaction #1, for example, when a gas-phase TiCl_4 attaches to the surface, a $\text{Ti}^*(\text{s})$ becomes buried and is thus now a bulk species instead. As a result, one bulk-phase atom is added to the solid for each one that arrives from the gas. A reverse process occurs in reaction #14.

Because the surface species are merely reaction intermediates, it is natural to assume that their concentrations will be at steady state. A conservation equation can then be written for each; however, since the total concentrations of titanium and nitrogen species are both conserved, only eight of the ten equations are independent. Denoting by R_i the rate (in $\text{mol}/\text{cm}^2\text{s}$) of reaction i , the equations can be written concisely as

$$R_1 + R_2 = R_3 + R_6 + R_7 = R_4 + R_8 + R_9 = R_5 + R_{10} + R_{11} = 3 R_{12} = 3 R_{13} = 6 R_{14} \equiv r \quad [2]$$

$$R_3 + R_4 + R_5 = R_1 + R_6 + R_8 + R_{10} = R_2 + R_7 + R_9 + R_{11} \equiv s \quad [3]$$

The net production rates of the gaseous and bulk species are then

$$\begin{aligned}
\text{HCl(g): } R_1 + R_2 + R_3 + \dots + R_{11} &= 3s = 4r \\
\text{TiCl}_4\text{(g): } -R_1 - R_2 &= -r \\
\text{NH}_3\text{(g): } -R_3 - R_4 - R_5 = -s &= -\frac{4}{3}r \\
\text{N}_2\text{(g): } R_{14} &= \frac{1}{6}r \\
\text{Ti(d): } R_1 + R_2 &= r \\
\text{N(d): } R_3 + R_4 + R_5 - 2R_{14} = s - \frac{1}{3}r &= r
\end{aligned}$$

Comparing with Eq. [1], it can be seen that the surface mechanism reproduces exactly the stoichiometry of the overall reaction.

Next, the kinetic law for the process can be derived by inserting expressions for the rates of the individual steps into Eqs. [2] and [3], assuming mass-action kinetics in each case. For simplicity, the rate constants will be taken to be equal for all reactions within a given group; the values for the five groups will be denoted by α , β , γ , λ , and δ , respectively. The goal is to write the overall deposition rate r in terms of these rate constants and the concentrations C_{TiCl_4} and C_{NH_3} of the gas-phase reactants. Since the concentration of N(b) is a constant, it can be incorporated into the rate constant δ with no loss of generality. In order to eliminate the concentrations of the ten surface species, one can use the eight conservation equations together with the condition that the total concentrations of Ti- and N-containing species are each equal to 1/2 of the overall surface site density ρ . After a fair amount of algebra, the following expression for the deposition rate is obtained:

$$r = \frac{3\lambda}{4(\phi_n + 2)^2} \left\{ \left[\frac{\lambda}{2\delta} + \rho^2 \frac{(\phi_n + 2)\theta\phi_t\phi_n}{1 + \phi_t + \theta\phi_t\phi_n} \right]^{1/2} - \left(\frac{\lambda}{2\delta} \right)^{1/2} \right\}^2 \quad [4]$$

where $\phi_t = (5\alpha/3\gamma) C_{\text{TiCl}_4}$, $\phi_n = (5\beta/4\gamma) C_{\text{NH}_3}$, and $\theta = \gamma/5\lambda$. Needless to say, the way in which the deposition rate varies with the reactant concentrations is, according to Eq. [4], rather complicated. However, the behavior in various limiting cases is simple and physically realistic. For example, if ϕ_t and ϕ_n are both arbitrarily small, then

$$r \doteq \frac{25}{384} \delta \left(\frac{\alpha\beta\rho^2}{\gamma\lambda} \cdot C_{\text{TiCl}_4} \cdot C_{\text{NH}_3} \right)^2 \quad [5]$$

and the overall reaction is second-order in each reactant. On the other hand, if ϕ_n is arbitrarily small but $\phi_t \gg 1$, then

$$r \doteq \frac{3}{128} \delta \left(\frac{\beta\rho^2}{\lambda} \cdot C_{\text{NH}_3} \right)^2 \quad [6]$$

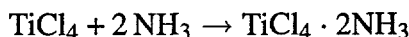
so that the reaction is still second-order in NH_3 but now zeroth-order in TiCl_4 . This accords reasonably well with the results that have been reported in the literature (3,4); a small negative order in TiCl_4 is actually observed, but this has been attributed to competing gas-phase complex formation. In any case, it should be noted that Eq. [6] does not involve the rate constants α and γ , which may therefore be difficult to determine.

EVALUATION OF RATE CONSTANTS

Since there are currently no methods available for calculating α , β , γ , λ , and δ from first principles, the only option is to infer them from experimental data for the overall deposition rate. Of course, this rate is invariably reported as a function of the inlet gas composition, while the surface

mechanism is written in terms of local concentrations. In order to account for such effects as mass transport and reactant depletion, one must use the mechanism in conjunction with a computational reactor model. Unfortunately, literature studies generally fail to specify some key parameters, such as the surface/volume ratio and the residence time, that would be necessary input to a reactor simulation. The only data set for which such information is available is that generated recently at Sandia/New Mexico in an MRC rotating disk reactor (11). Therefore, this data will be used to determine the rate constants in the analysis to follow.

As noted above, the expression in Eq. [4] is at worst of order 0 in TiCl_4 , whereas most experimental studies show a small negative order. This has been attributed to a competing gas-phase reaction that produces the (possibly) nonreactive complex $\text{TiCl}_4 \cdot 2\text{NH}_3$ (3). Therefore, the surface mechanism will be augmented here with the homogeneous reaction



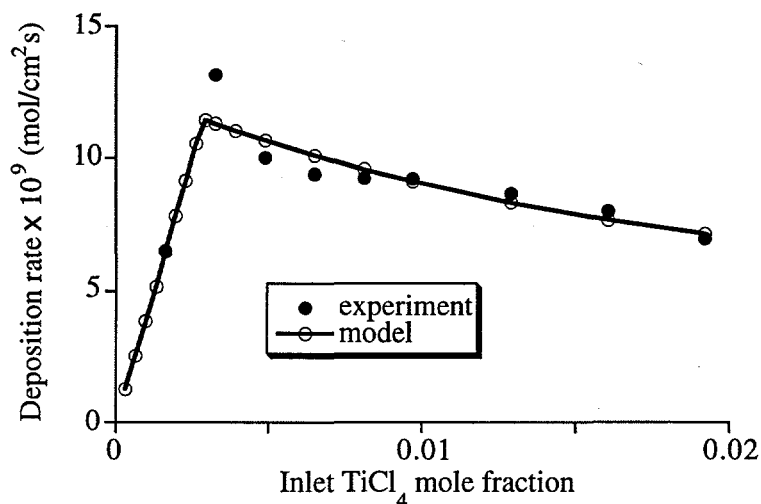
having a third-order rate constant k . The supposition is that an increasing inlet concentration of TiCl_4 causes additional NH_3 to be tied up in complexes and thus decreases the deposition rate, which is generally observed to have a strong positive order in NH_3 .

In the Sandia study, the deposition rate was measured as a function of the inlet concentration of TiCl_4 but not NH_3 . Furthermore, experiments were carried out at only one substrate temperature (903 K), so all computed surface rate constants will refer to this temperature. However, there was a substantial temperature gradient between the substrate and the inlet showerhead (at 623 K), so an activation energy E will be used in conjunction with the gas-phase rate constant k . There are thus 7 adjustable parameters to be determined by optimizing the fit to the experimental deposition rates over the entire range of TiCl_4 concentrations. For any given set of parameters, the predicted deposition rates are computed from Sandia's SPIN code (12). The pressure is in all cases fixed at 20 Torr, the inlet NH_3 mole fraction varies slightly from 0.0196 to 0.0192, and the value of ρ , as computed from the bulk density of TiN, is $3.61 \times 10^{-9} \text{ mol/cm}^2$.

The optimized fit to the rotating disk reactor data is shown in Figure 1. The root-mean-square relative deviation between the experimental and theoretical values is 6.19%, which is probably within the uncertainty in the data. The near-kink in the model curve is highly unusual but seems to be real, as opposed to simply a numerical artifact. On the initial, rising portion of the curve, the TiCl_4 concentration at the substrate is reduced so severely that the intrinsic deposition rate is no longer in the zero-order regime, and the deposition is limited by the supply of this reactant. On the remainder of the curve, depletion of TiCl_4 is no longer an issue, and the deposition rate falls slowly due to the effect of the gas-phase complexing reaction.

Since the experimental data set does not span a wide range of process conditions, it is perhaps not surprising that the data fitting procedure does not provide definite values for all of the unknown rate parameters. The optimum value of α is essentially infinite, which suggests that Ti deposition is so efficient that it rarely limits the overall process. Likewise, the quality of the data fit is extremely insensitive to the value of γ , as long as it is large enough that ϕ_n is generally much smaller than unity, yet small enough that ϕ_t is generally large. The optimized values for the remaining rate constants are less uncertain: $\beta = (6.86 \pm 0.30) \times 10^{19} \text{ cm}^5/\text{mol}^2\text{s}$, $\lambda = (5.77 \pm 0.29) \times 10^{10} \text{ cm}^2/\text{mol} \cdot \text{s}$, $\delta = (5.13 \pm 0.21) \times 10^{26} \text{ cm}^6/\text{mol}^3\text{s}$, $k = (2.59 \pm 0.53) \times 10^{18} \text{ cm}^6/\text{mol}^2\text{s}$, and $E = (76.0 \pm 13.2) \text{ kcal/mol}$. The quoted uncertainties are arbitrarily chosen to be those perturbations that cause the quality of the data fit to be degraded from 6.19% to 7%; this is enough to give rise to a noticeable change. The value given for β can be shown to correspond to a reactive sticking coefficient of 0.0332 for NH_3 .

Figure 1. Optimized fit of deposition data from Sandia/MRC rotating disk reactor



The value of E is unrealistically large and has the effect of essentially confining the complexing reaction to the immediate vicinity of the substrate. This suggests that the source of the negative reaction order in TiCl_4 may actually be a heterogeneous reaction after all.

As noted earlier, lack of information about some reactor parameters makes it impossible to perform a rigorous analysis of the experimental data available in the literature. However, if it is assumed that the experiments were carried out under differential conditions, i.e., in the absence of significant reactant depletion (as claimed in Reference 4, for example), then the analysis becomes feasible. The data in References 3 and 4 are a natural choice to use, since they refer to temperatures close to that used in the Sandia study (although the pressures are lower by two orders of magnitude). Rather than re-optimizing the rate constants, however, we choose to keep those already computed and simply *predict* the deposition rates for the "new" data sets. In order to provide a fair comparison, the experimental values are first adjusted to 903 K by using the activation energies quoted in the respective articles.

The results of this procedure are shown in Figures 2–4. It can be seen that the predicted deposition rates are always within a factor of two of the observed values and usually much closer than that; in fact, for the near-differential reactor experiments of Srinivas et al. (4), the deviation never exceeds 40%. Since this kind of treatment necessarily ignores the depletion effect of the complexing reaction, the observed negative reaction orders in TiCl_4 cannot be reproduced; the predicted order is essentially zero. Not surprisingly, this is a more serious problem for the experimental conditions of Buiting et al. (3). On the other hand, the observed trends in the deposition rate with NH_3 concentration are predicted quite well. This kind of agreement may be partly fortuitous if the reactor experiments were not truly differential, as suggested by the TiCl_4 results. Nevertheless, the overall success of the model gives considerable support to the proposed surface reaction mechanism.

Figure 2. Predicted vs. observed deposition rates (adjusted to 903 K) in experiments of Buiting

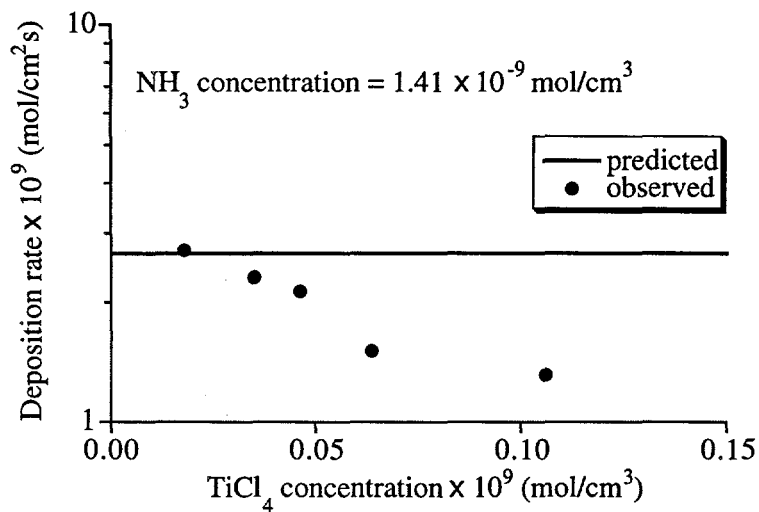


Figure 3. Predicted vs. observed deposition rates (adjusted to 903 K) in experiments of Srinivas

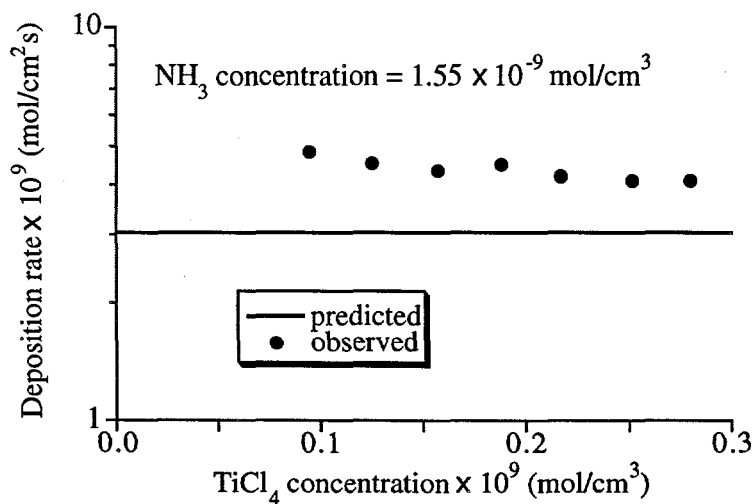
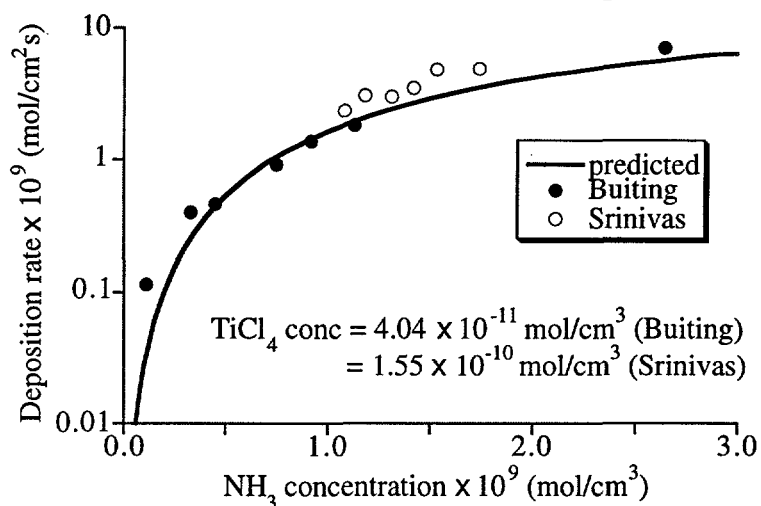


Figure 4. Predicted vs. observed deposition rates (adjusted to 903 K) in two sets of experiments



REFERENCES

1. A. Intemann, H. Koerner, and F. Koch, *J. Electrochem. Soc.*, **140**, 3215 (1993).
2. J. B. Price, J. O. Borland, and S. Selbrede, *Thin Solid Films*, **236**, 311 (1993).
3. M. J. Buiting, A. F. Otterloo, and A. H. Montree, *J. Electrochem. Soc.*, **138**, 500 (1991).
4. D. Srinivas, J. T. Hillman, W. M. Triggs, and E. C. Eichman, in *Advanced Metallization for ULSI Applications/1991*, V. V. S. Rana, R. V. Joshi, and I. Ohdomari, Editors, p. 319, Materials Research Society, Pittsburgh, PA (1992).
5. M. J. Buiting and A. F. Otterloo, *J. Electrochem. Soc.*, **139**, 2580 (1992).
6. C.-C. Jiang, T. Goto, and T. Hirai, *J. Mater. Sci.*, **28**, 6446 (1993).
7. Y. Ohshita, W. Fukagawa, and A. Kobayashi, *J. Crystal Growth*, **146**, 188 (1995).
8. M. Nadal and F. Teyssandier, *J. Physique IV, Colloque C5*, 809 (1995).
9. Y. Mochizuki, Y. Okamoto, A. Ishitani, K. Hirose, and T. Takada, *Jpn. J. Appl. Phys.*, **34**, L326 (1995).
10. M. D. Allendorf, C. L. Janssen, M. E. Colvin, C. F. Melius, I. M. B. Nielsen, T. H. Osterheld, and P. Ho, in *Process Control, Diagnostics, and Modeling in Semiconductor Manufacturing*, vol. 95-2, p. 393, The Electrochemical Society, Pennington, NJ (1995).
11. J. S. Custer and P. M. Smith, unpublished data.
12. M. E. Coltrin, R. J. Kee, G. H. Evans, E. Meeks, F. M. Rupley, and J. F. Grcar, Sandia National Laboratories Report SAND91-8003 (1991).

UNLIMITED RELEASE
INITIAL DISTRIBUTION

Dr. Peter Angelini
Building 4515
Oak Ridge National Laboratory
P.O. Box 2008, 1 Bethel Valley Road
Oak Ridge, TN 37831-6065

Dr. Sara Dillich
Adv. Industrial Concepts Div., EE-232
U.S. DOE - EE
Forrestal Building
1000 Independence Avenue
Washington, DC 20585

Dr. Charles A. Sorrell
Adv. Industrial Concepts Div., EE-232
U.S. DOE - EE
Forrestal Building
1000 Independence Avenue
Washington, DC 20585

Dr. Theodore M. Besmann
Oak Ridge National Laboratory
P.O. Box 2008
Oak Ridge, TN 37831-6063

Dr. F. D. Gac
G771
Los Alamos National Laboratory
P.O. Box 1663
Los Alamos, NM 87545

Dr. Greg Glaitzmaier
NREL
1617 Cole Blvd.
Golden, CO 80401

Dr. Suleyman A. Gokoglu
NASA Lewis Research Center
Mail Stop 106-1
Cleveland, OH 44135

Dr. Michael Zachariah
National Institute of Standards and Technology
Building 221, Rm. B312
Gaithersburg, MD 20899

Dr. John W. Hastie
National Institute of Standards and Technology
Metallurgy Division
B106/223
Gaithersburg, MD 20899

Dr. Gerd M. Rosenblatt
Building 50A, Room 4119
Lawrence Berkeley Laboratory
1 Cyclotron Road
Berkeley, CA 94720

Prof. Peter B. Armentrout
Dept. of Chemistry
University of Utah
Henry Eyring Building
Salt Lake City, UT 84112

Prof. Richard Axelbaum
Dept. of Mechanical Engineering
Washington University
St. Louis, MO 63130

Prof. Dieter Baeuerle
Johannes-Kepler-Universitat Linz
Institut für Angewandte Physik
A-4040 Linz
AUSTRIA

Prof. C. Bernard
Laboratoire de Thermodynamique
ENSEEG
BP.75,38402
St. Martin d'Hères
FRANCE

Prof. John I. Brauman
Dept. of Chemistry
Stanford University
Stanford, CA 94305

Dr. Ken Brezinsky
Dept. of Mechanical and Aerospace
Engineering
Princeton University
Engineering Quadrangle, D329
Princeton, NJ 08544

Prof. Mark A. Capelli
Dept. of Mechanical Engineering
Stanford University
Building 500
Stanford, CA 94305-1901

Prof. Jan-Otto Carlsson
Uppsala University
Chemistry Dept.
Box 531
S-75121 Uppsala
SWEDEN

Prof. David S. Dandy
Dept. of Agricultural and Chemical
Engineering
Colorado State University
Fort Collins, CO 80523

Prof. Robert F. Davis
Dept. of Materials Science and
Engineering
North Carolina State University
229 Riddick Laboratories
Raleigh, NC 27695

Prof. Seshu B. Desu
Dept. of Materials Science and
Engineering
Virginia Polytechnic Institute
213 Holden Hall
Blacksburg, VA 24061-0140

Prof. James Edgar
Dept. of Chemical Engineering
Kansas State University
Manhattan, KS 66506-5102

Prof. James W. Evans
Dept. of Materials Science and Mineral Engineering
University of California
Berkeley, CA 94720

Prof. Richard C. Flagan
Environmental Engineering
California Institute of Technology
138-78
Pasadena, CA 91125

Prof. Arthur Fontijn
Dept. of Chemical Engineering
Rensselaer Polytechnic Institute
110 8th Street
Troy, NY 12180-3590

Prof. Michael Frenklach
Dept. of Materials Science and Engineering
Pennsylvania State University
202 Academic Projects Building
University Park, PA 16802

Prof. Bernard Gallois
Dept. of Materials Science
Stevens Institute of Technology
Castle Point on the Hudson
Hoboken, NJ 07030

Dr. Robert H. Hauge
Dept. of Chemistry
Rice University
Houston, TX 77251

Prof. Peter Hess
Institut für Physikalische Chemie
Heidelberg University
Im Neuenheimer Feld 253
69120 Heidelberg
GERMANY

Prof. D. Lynn Johnson
Dept. of Materials Science and
Engineering
Northwestern University
The Technological Institute
Evanston, IL 60201

Prof. Linda Jones
NYS College of Ceramics
Alfred University
2 Pine Street
Alfred, NY 14802

Prof. Joseph L. Katz
Chemical Engineering
Johns Hopkins University
Charles and 34th Streets
Baltimore, MD 21218

Prof. Keith King
Dept. of Chemical Engineering
University of Adelaide
Adelaide, SA
AUSTRALIA 5005

Prof. H. Komiyama
Dept. of Chemical Engineering
University of Tokyo
Hongo 7, Bunkyo-ku
Tokyo 113
JAPAN

Dr. F. Langlais
Laboratoire des Composites
Thermostructuraux
Domaine Universitaire
33600 Pessac
FRANCE

Prof. M.C. Lin
Dept. of Chemistry
Emory University
Atlanta, GA 30322

Prof. Paul Marshall
Dept. of Chemistry
University of North Texas
P.O. Box 5068
Denton, TX 76203-5068

Prof. R. E. Mitchell
Dept. of Mechanical Engineering
Stanford University
Stanford, CA 94305

Prof. Philip W. Morrison, Jr.
Dept. of Chemical Engineering
Case Western Reserve University
10900 Euclid Avenue
Cleveland, OH 44106-7217

Prof. Triantafillos J. Mountziaris
Chemical Engineering Dept.
SUNY Buffalo
Buffalo, NY 14260

Prof. Zuhair A. Munir
Dept. of Mechanical Engineering
University of California
Davis, CA 95616

Prof. Clifford E. Myers
State University of New York at Binghamton
Dept. of Chemistry
Binghamton, NY 13901

Dr. Roger Naslain
Laboratoire des Composites Thermostructuraux
Domaine Universitaire
33600 Pessac
FRANCE

Dr. Michel Pons
Laboratoire de Science des Surfaces et
Matériaux Carbonés
Institut National Polytechnique de Grenoble
ENSEEG
38402 Saint-Martin-d'Herès Cedex
FRANCE

Prof. S. E. Pratsinis
Chemical and Nuclear Engineering
University of Cincinnati
627 Rhodes Hall, Mail Loc. 171
Cincinnati, OH 45221-0171

Prof. Daniel E. Rosner
Chemical Engineering Dept.
Yale University
P.O. Box 2159, Yale Station
New Haven, CT 06520-2159

Prof. Adel Sarofim
Dept. of Chemical Engineering
Massachusetts Institute of Technology
66-466
Cambridge, MA 02139

Prof. Brian W. Sheldon
Division of Engineering
Brown University
Box D
Providence, RI 02912

Dr. Daniel J. Skamser
Dept. of Materials Science and Engineering
Northwestern University
MLSF 2036
Evanston, IL 60208-3108

Prof. Stratis V. Sotirchos
Dept. of Chemical Engineering
University of Rochester
Rochester, NY 14627-0166

Prof. Karl E. Spear
Dept. of Ceramic Science and Engineering
Pennsylvania State University
201 Steidle Building
University Park, PA 16802

Prof. Thomas L. Starr
Room 113
Baker Building
Georgia Institute of Technology
Atlanta, GA 30332-0245

Prof. Stan Veprek
Institute of Chemistry of Information Recording
Technical University of Munich
Lichtenbergstrasse 4
D-8046 Barching-Munich
GERMANY

Dr. Thomas H. Baum
Advanced Technology Materials
7 Commerce Drive
Danbury, CT 06810-4169

Dr. H. F. Calcote
Director of Research
Aerochem Research Laboratories
P.O. Box 1
Princeton, NJ 08542

Dr. Douglas W. Freitag
DuPont Lanxide Composites, Inc.
17 Rocky Glen Court
Brookeville, MD 20833

Dr. Jitendra S. Goela
Morton Advanced Materials
185 New Boston Street
Woburn, MA 01801-6278

Dr. Christopher J. Griffin
3M Corporation
3M Center, Building 60-1N-01
St. Paul, MN 55144-1000

Dr. Stephen J. Harris
Physical Chemistry Dept.
GM Research and Development
30500 Mound Road 1-6
Warren, MI 48090-9055

Dr. Bruce H. Weiller
Mechanics and Materials Technology Center
Aerospace Corporation
P.O. Box 92957
Los Angeles, CA 90009-2957

Dr. James Loan
MKS Instruments, Inc.
6 Shattuck Road
Andover, MA 01810

Dr. K. L. Luthra
General Electric Corporate Research and
Development
Room 3B4, Building K1
Schenectady, NY 12301

Dr. Richard J. McCurdy
Libbey-Owens-Ford Co.
1701 East Broadway
Toledo, OH 43605

Dr. Meyya Meyyappan
Scientific Research Associates
50 Nye Road
Glastonbury, CT 06033

Dr. Thomas H. Osterheld
Applied Materials, Inc.
Mail Stop 1510
Santa Clara, CA 95054

Mr. Peter Reagan
Project Manager, CVD Composites
ThermoTrex Corporation
74 West Street, P.O. Box 9046
Waltham, MA 02254-9046

Dr. David Roberts
J. C. Schumacher
1969 Palomar Oaks Way
Carlsbad, CA 92009

Dr. Andrew J. Sherman
Ultramet
12173 Montague Street
Pacoima, CA 91331

Dr. Richard Silbergliitt
Technology Assessment and Transfer, Inc.
133 Defense Highway, #212
Annapolis, MD 21401

Dr. Mark H. Headinger
DuPont Lanxide Composites, Inc.
400 Bellevue Road, P.O. Box 6100
Newark, DE 19714-6100

MS 0457 R. J. Eagan, 1000

MS 0601 W. G. Breiland, 1126

MS 0601 M. E. Coltrin, 1126

MS 0601 P. Esherick, 1126

MS 0601 P. Ho, 1126

MS 0601 H. K. Moffat, 1126

MS 0702 D. E. Arvizu, 6200

MS 0710 G. A. Carlson, 6211

MS 1077 L. M. Cecchi, 1326

MS 1078 H. T. Weaver, 1321

MS 1079 A. D. Romig, 1300

MS 1084 J. S. Custer, 1323

MS 1084 P. M. Smith, 1323

MS 1349 R. E. Loehman, 1808

MS 1380 D. W. Schaefer, 4200

MS 1417 S. T. Picraux, 1112

MS 9001 T. O. Hunter, 8000
Attn: L. A. West, 8200
R. C. Wayne, 8400

MS 9042 C. M. Hartwig, 8345
Attn: G. H. Evans
S. K. Griffiths
W. G. Houf
R. H. Nilson

MS 9042 R. J. Kee, 8303

MS 9042 R. S. Larson, 8345 (10)

MS 9042 E. Meeks, 8345

MS 9052 M. D. Allendorf, 8361 (15)

MS 9052 D. R. Hardesty, 8361

MS 9054 W. J. McLean, 8300
Attn: C. W. Robinson, 8301
W. Bauer, 8302
L. A. Rahn, 8351
G. A. Fisk, 8355
R. W. Carling, 8362
R. J. Gallagher, 8366

MS 9055 F. P. Tully, 8353

MS 9141 T. M. Dyer, 8700
Attn: M. W. Perra, 8711
M. I. Baskes, 8712
M. C. Nichols, 8715

MS 9161 R. H. Stulen, 8250

MS 9161 W. G. Wolfer, 8717

MS 9162 D. A. Outka, 8716

MS 9162 A. E. Pontau, 8347

MS 9162 M. T. Schulberg, 8716

MS 9214 C. F. Melius, 8117

MS 9021 Technical Communications Dept., 8815,
for OSTI (2)

MS 9021 Technical Communications Dept., 8815/
Technical Library, MS 0899, 4414

MS 0899 Technical Library, 4414 (4)

MS 9018 Central Technical Files, 8950 (3)